PROCEEDINGS OF SPIE

SPIEDigitalLibrary.org/conference-proceedings-of-spie

Fiber-based two-wavelength heterodyne displacement interferometer

Yanqi Zhang, Ki-Nam Joo, Felipe Guzman

Yanqi Zhang, Ki-Nam Joo, Felipe Guzman, "Fiber-based two-wavelength heterodyne displacement interferometer," Proc. SPIE 12008, Photonic Instrumentation Engineering IX, 120080K (5 March 2022); doi: 10.1117/12.2609998

SPIE.

Event: SPIE OPTO, 2022, San Francisco, California, United States

Downloaded From: https://www.spiedigitallibrary.org/conference-proceedings-of-spie on 29 Jun 2022 Terms of Use: https://www.spiedigitallibrary.org/terms-of-use

Fiber-based two-wavelength heterodyne displacement interferometer

Yanqi Zhang[a,b], Ki-Nam Joo[c], Felipe Guzman*[a]
[a]Dept. of Aerospace Engineering, Texas A&M Univ., 701 H.R. Bright Bldg., College Station, TX USA 77843-3141; [b]Wyant College of Optical Sciences, Univ. of Arizona, 1630 E. Univ. Blvd., Tucson, AZ USA 85721; [c]Dept. of Photonic Engineering, Chosun Univ., 309 Pilmun-daero, Dong-gu, Gwangju 61452, Republic of Korea

ABSTRACT

Precision displacement laser interferometry is crucial in various applications such as microlithography, high-performance profilometry, and gravitational wave detection. We are currently developing a fiber-based heterodyne laser interferometer that features compact size and low noise floor. Laser beams at two different wavelengths are utilized to construct a fiber-based interferometer system. Narrow band spectral filters are used to separate the beams of different wavelengths and to control their optical paths. The highly common optical paths between the two interferometers provide a high common-mode rejection ratio to instrument and environmental noise sources. In this paper we present the interferometer design, benchtop prototype system, and preliminary measurement results obtained in the lab environments. A benchtop prototype shows sub-nm/√Hz displacement sensitivities in air at frequencies above 100 mHz in our lab.

Keywords: Displacement measuring interferometry (DMI), heterodyne interferometer, common-mode rejection, noise suppression

1. INTRODUCTION

Displacement measuring interferometry (DMI) has been extensively applied in precision engineering as a metrology tool in a vast number of applications, such as semiconductor inspection and non-contact surface profilometry. In the past decades, DMI has extended its application to optomechanical inertial sensing [1] and gravitational wave (GW) detection [2-5], where the design and development of DMI techniques are facing various challenges. In optomechanical inertial sensing, DMI is used as an optical readout system to measure the test mass displacement, from which the acceleration is determined by the inherent transfer function of the mechanical resonator [1]. In GW detection, DMI has been applied to measure free-falling test mass at the Laser Interferometric Space Antenna (LISA) [2-5], and to measure the intersatellite displacement in the mission GRACE Follow-On [6, 7]. The applications of DMI in both areas require a high sensitivity of picometer level in the low frequency regime between micro-Hz to a few Hz. In this regime, typical noise sources such as laser frequency noise and temperature fluctuations become non-negligible [8-10], resulting in an increasing noise floor towards low frequencies. The overall footprint of a DMI system has also increasingly become one of the major design considerations, especially for portable systems and space missions, due to their limited budget for volume and mass. In addition, target displacements can range from a few micrometers to several millimeters, raising challenges of large measurement range for the DMI system.

Among various DMI techniques, heterodyne interferometry provides key features such as large measurement range, inherent directionality, and fast detection speed. The DMI systems in LISA and its technology demonstrator LISA Pathfinder are developed based on heterodyne interferometry [11-13]. The overall system design follows a common-mode rejection design scheme, where reference interferometers with common optical paths are integrated on the same baseplate with the main displacement measuring interferometer to effectively mitigate environmental noises. However, the development of the interferometer unit needs demanding fabrication, alignment, and bonding techniques. Recently, the advancement of compact heterodyne laser interferometer with common-mode design [14] shows its potential in inertial sensing area. Simple system design reduces the overall system footprint while maintaining the integration of reference interferometer to reject environmental noises. The investigation of noise sources [15] shows that the detection sensitivity can be enhanced by performing post-signal processing algorithms without additional complexity in the instrumentation. However, the performance of the overall system greatly depends on the manufacturing tolerance and alignment of individual component, as well as the long-term stability of the adhesives and the overall assembly.

*felipe@tamu.edu

Photonic Instrumentation Engineering IX, edited by Lynda E. Busse, Yakov Soskind, Proc. of SPIE Vol. 12008, 120080K · © 2022
SPIE · 0277-786X · doi: 10.1117/12.2609998

Downloaded From: https://www.spiedigitallibrary.org/conference-proceedings-of-spie on 29 Jun 2022
Terms of Use: https://www.spiedigitallibrary.org/terms-of-use

In this paper, we present a design of a fiber-based heterodyne displacement laser interferometer that uses two wavelengths as the optical sources. The system takes advantage of a common-mode heterodyne interferometer design to increase the measurement range as well as to reduce the noises in the low frequency regime, aiming at picometer level sensitivity in the sub-Hz frequency bandwidth. In the proposed system, the common-mode design is achieved by using two lasers whose wavelengths are tens of nanometers apart. Each laser source constructs one heterodyne interferometer. The optical paths of the two interferometers overlap in most of the system until they are separated by a spectral filter before the target mirror. This way one interferometer serves as the reference interferometer to monitor the noise sources in the system, and the other is the main interferometer that measures the test mass displacement. Furthermore, the overall system is compact due to the flexibility in packaging fiber components. In this paper, Section 2 introduces the system design in detail and the principles of the phase measurement. The benchtop prototype system and preliminary test results are presented in Section 3, where the sensitivity floor is measured to be 7.6×10^{-12} m/√Hz at 100 mHz in air.

2. SYSTEM DESIGN

2.1 Two-wavelength heterodyne interferometer

In a heterodyne displacement laser interferometer, acousto-optic modulators are usually used to shift the laser frequencies by several kHz to several MHz, to create a slight frequency difference between two interfering beams. The interference is detected by a photodetector (PD), where the irradiance can be generally expressed as

$$I = I_0[1 + V\cos(2\pi f_{het}t + \phi)], \tag{1}$$

where I_0 is the nominal optical power, f_{het} denotes the heterodyne frequency that is the frequency difference between two interfering beams. Moreover, V is the visibility of the interferometer, and displacement of the target is reflected in the phase term ϕ. Various methods can be used to extract the phase ϕ from detected irradiance such as a phase locked loop (PLL) [16], or single-bin Fourier transform [11]. In a double-pass interferometer, the target displacement d is calculated from the phase term following

$$d = \frac{\phi}{2\pi\cdot 2}\cdot\lambda, \tag{2}$$

where λ is the nominal wavelength of the laser.

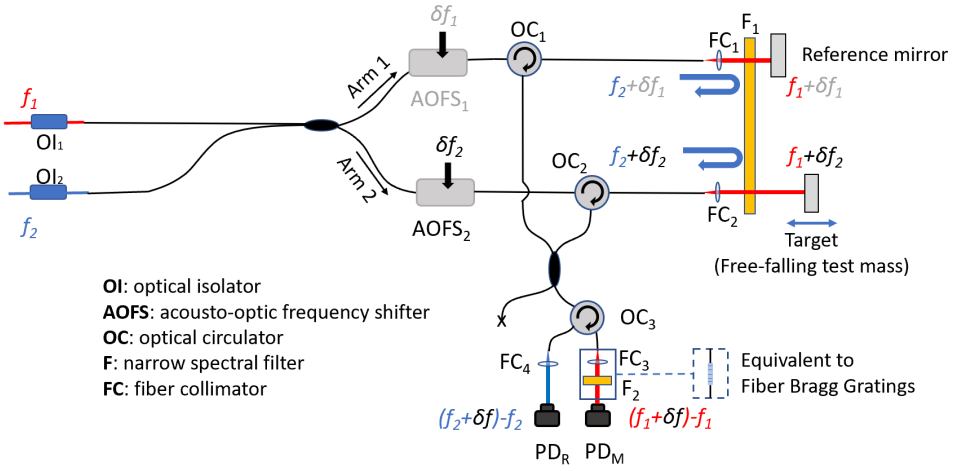

Figure 1. System layout of the two-wavelength fiber-based heterodyne displacement interferometer. Two laser sources are applied to construct two individual heterodyne interferometers in one system, whose optical paths are separated by a narrow-bandwidth spectral filter. One interferometer is used to measure the test mass displacement and the other is to monitor the environmental noises.

Figure 1 shows the system layout of the proposed two-wavelength heterodyne interferometer. Two laser sources running at different wavelengths λ_1 and λ_2, are used to construct two individual heterodyne interferometers in the system. The two interferometers share common optical paths until λ_2 is reflected by a spectral filter while λ_1 transmits through. The λ_2 interferometer is used to monitor the system noises while the λ_1 interferometer is used to measure the test mass displacement. In the detection part, the irradiances of two interferometers are also separated by a spectral filter and directed

Downloaded From: https://www.spiedigitallibrary.org/conference-proceedings-of-spie on 29 Jun 2022
Terms of Use: https://www.spiedigitallibrary.org/terms-of-use

to corresponding photodetectors. The actual displacement measurement with enhanced sensitivity can be calculated by subtracting the noise readout from the test mass motion readout.

The output beams from two lasers are mixed and split into two interferometer arms. In each arm, both optical frequencies are shifted by the acousto-optic frequency shifter (AOFS) with the same shifting frequency. In arm 1, when entering optical circulator (OC) through port 1, beams are directed to exit through port 2 towards the measurement end. After the fiber collimator, a spectral filter with narrow bandwidth is inserted to separate two laser wavelengths. The beam with wavelength λ_2 is reflected by the spectral filter, entering port 2 of the OC, and directed to port 3 of the OC where it is combined with the beam of same wavelength λ_2 in arm 2. This λ_2 interferometer is called the reference interferometer (RIFO), mainly for noise measurement. Back to arm 1, at the surface of spectral filter, the beam with wavelength λ_1 is transmitted through and incident on the fixed reference mirror. Similarly, after reflected by the reference mirror, this beam exiting port 3 of OC is combined with the beam of wavelength λ_1 from arm 2, constructing the measurement interferometer (MIFO) that measures the test mass displacement. In the detection part, another spectral filter is used to separate the irradiance for two individual interferometers. Alternatively, a fiber Bragg grating (FBG) can be used instead of the spectral filter for a more compact system. However, the FBG can only be used in the detection part to substitute the spectral filter F_2 but not in the measurement end for F_1, as the filter F_1 needs to be as closed to the target and reference mirrors as possible to maximize the common mode optical paths between MIFO and RIFO.

The two laser wavelengths are selected so that the difference between them is large enough to be separated by the spectral filter with a narrow bandwidth, which is usually a few nanometers. Also, the frequency difference needs to be small enough so that the dispersion effects and transmission loss in the fiber components are negligible. For polarization-maintaining fiber (PMF) components, this bandwidth limit is usually 10 to 20 nm.

This interferometer is based on fiber components so that the overall packaging size can be compact. The use of all-fiber components minimizes free-beam alignment efforts during system assembly.

2.2 Displacement measurement

Both MIFO and RIFO are heterodyne interferometers but running at different laser wavelengths. The heterodyne frequencies of the two interferometers are the same where $f_{het} = \delta f_2 - \delta f_1$, and δf_i is the shifted frequency by corresponding AOFS in the i_{th} arm. In this case, based on Equation 1, the detected irradiance for MIFO and RIFO are represented as

$$I_M = I_{M0}[1 + V_M \cos(2\pi f_{het} t + \phi_M)], \tag{3}$$

$$I_R = I_{R0}[1 + V_R \cos(2\pi f_{het} t + \phi_R)]. \tag{4}$$

The phase term ϕ_R in RIFO includes the optical path difference (OPD) between arm 1 and 2 before the spectral filter surface, where $\Delta\phi_{0R} = \phi_{2R} - \phi_{1R}$, and the fluctuations in the phase difference between two arms due to environmental noises, where $\Delta\phi_{NR} = \phi_{N2R} - \phi_{N1R}$. The phase term ϕ_M in MIFO also includes nominal OPD term $\Delta\phi_{0M}$ and noise fluctuations $\Delta\phi_{NM}$ because the optical paths are common between these two interferometers before the spectral filter. Besides, ϕ_M also includes the phase variation due to the displacement of the target mirror with respect to the reference mirror, $\Delta\phi_{2M} - \Delta\phi_{1M}$, as shown in Figure 2. In summary, the phase terms in MIFO and RIFO can be decomposed as

$$\phi_R = (\phi_{2R} - \phi_{1R}) + (\phi_{N2R} - \phi_{N1R}) = \Delta\phi_{0R} + \Delta\phi_{NR}, \tag{5}$$

$$\phi_M = \Delta\phi_{0M} + \Delta\phi_{NM} + \Delta\phi_{2M} - \Delta\phi_{1M}. \tag{6}$$

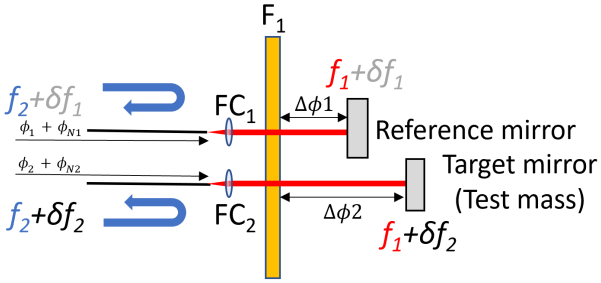

Figure 2. Zoom-in view of two arms on the measurement end in the two-wavelength interferometer.

Downloaded From: https://www.spiedigitallibrary.org/conference-proceedings-of-spie on 29 Jun 2022
Terms of Use: https://www.spiedigitallibrary.org/terms-of-use

The actual displacement of the target mirror can be calculated from the differential phase between two interferometer readouts. Different wavelengths need to be taken into consideration when converting from phase to length. The displacement of the target mirror L is expressed as

$$\begin{aligned} L &= \frac{\Delta\phi_{2M} - \Delta\phi_{1M}}{2\pi} \cdot \lambda_1 \\ &= \left(\frac{\Delta\phi_{0M} + \Delta\phi_{NM}}{2\pi} \cdot \lambda_1 - \frac{\Delta\phi_{0R} + \Delta\phi_{NR}}{2\pi} \cdot \lambda_2\right) + \frac{\Delta\phi_{2M} - \Delta\phi_{1M}}{2\pi} \cdot \lambda_1 \\ &= \frac{\phi_M}{2\pi} \cdot \lambda_1 - \frac{\phi_R}{2\pi} \cdot \lambda_2 \end{aligned} \tag{7}$$

where λ_1 and λ_2 are the wavelengths of two laser sources.

3. PROTOTYPING AND TEST

3.1 Benchtop system

Based on the design concept, a benchtop prototype of the proposed two-wavelength heterodyne interferometer is developed in our lab, as shown in Figure 3. Off-the-shelf optical and mechanical components are used in the prototype system. The laser wavelengths are 1064 nm and 1055 nm respectively, creating a 9 nm wavelength difference so that the beam paths from different lasers are separated by the spectral filter (EO 39-364) with a bandwidth of 5 nm. Two AOFS (G&H T-M150-0.4C2G-3-F2P) are used to shift the nominal laser frequencies by 150 MHz and 145 MHz individually, generating a heterodyne frequency of 5 MHz. On the measurement end, only one static mirror is used for the measurement and reference mirror, to characterize the system noise floor. The interference is detected by two photodetectors (Thorlabs PDA30B2), and a commercial phasemeter (Liquid Instruments Moku:Lab) is used to extract the phase by using PLL algorithms at a sampling frequency of 30.5 Hz.

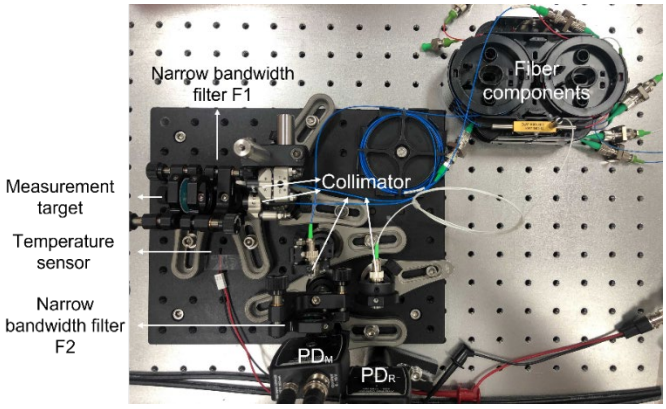

Figure 3. Benchtop system of the two-wavelength interferometer. The wavelengths are 1064 nm and 1055 nm. Off-the-shelf optical and mechanical components are used to construct this prototype system.

3.2 Preliminary test

Figure 4 shows the measurement results of MIFO, RIFO, and their differential measurement during an 8-hour preliminary test. The test is performed in an enclosed chamber under room temperature and 1 atmosphere pressure. In Figure 4 (a), the linear spectral density (LSD) of the displacement is plotted. The blue trace is under the orange trace due to the highly common optical paths shared between RIFO and MIFO. The logarithmic-average of the LSD plot shows a noise level of 3.7×10^{-10} m/√Hz at 100 mHz for individual interferometers RIFO and MIFO, while the noise level is reduced to 7.6×10^{-12} m/√Hz at 100 mHz for the differential measurement, which represents the actual noise floor of the overall system. Figure 4 (b) shows the displacement traces in time domain for the first 12 minutes of this measurement. The random drift of the individual interferometers has a peak-to-valley (PV) value of 5.72×10^{-6} m, while with the differential measurement, this random drift is reduced to 1.92×10^{-9} m. Both measurement results in the frequency and time domain indicate a significant reduction in the overall system noise level, which demonstrate the potentials in enhancing the detection sensitivity especially in the low frequency regime between 1 mHz to 1 Hz by applying the common-mode design scheme.

Downloaded From: https://www.spiedigitallibrary.org/conference-proceedings-of-spie on 29 Jun 2022
Terms of Use: https://www.spiedigitallibrary.org/terms-of-use

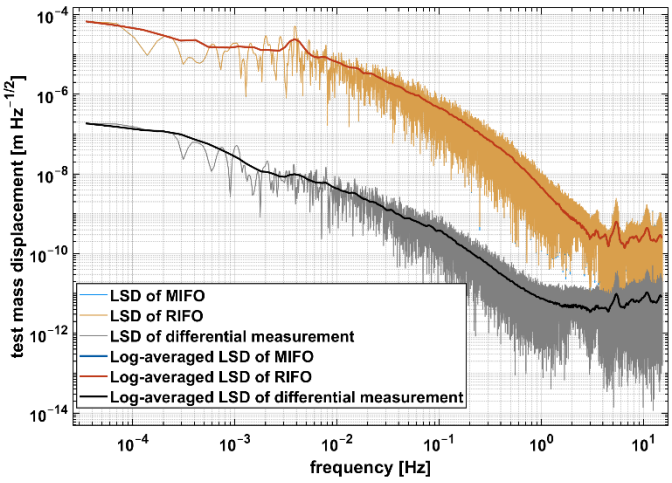

(a)

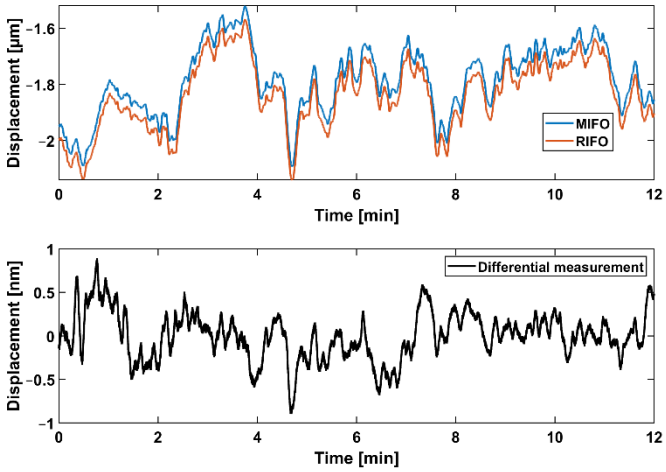

(b)

Figure 4. Preliminary test results for the benchtop prototype system in the lab environment. (a) Linear spectrum density (LSD) and logarithmic-averaged LSD of an 8-hour measurement for measurement interferometer (MIFO), reference interferometer (RIFO), and their differential measurement; (b) The first 12-mintue displacement traces of the measurement in (a) for MIFO, RIFO, and their differential measurement.

4. CONCLUSION

In this paper, we proposed a novel fiber-based heterodyne interferometer design to perform high-sensitivity displacement measurement. Due to the susceptibility of fiber components to the ambient noise sources such as thermal instability and vibrations, a common-mode design scheme is adopted to mitigate the environmental noise effects on the phase measurements. The common mode design is carried out by integrating two interferometers in the system, where one is served as the measurement interferometer to measure the test mass motion, and the other is served as the reference interferometer to monitor the system noises. The system sensitivity can therefore be enhanced by subtracting noise from the displacement measurement. The two interferometers utilize different wavelengths so that they share the same optical paths in the most part of the interferometer system but can be separated by a spectral filter before the target mirror.

Downloaded From: https://www.spiedigitallibrary.org/conference-proceedings-of-spie on 29 Jun 2022
Terms of Use: https://www.spiedigitallibrary.org/terms-of-use

The preliminary test results show a noise floor of 3.7×10^{-10} m/√Hz at 100 mHz for individual interferometers RIFO and MIFO, and a noise floor of 7.6×10^{-12} m/√Hz at 100 mHz for the differential measurement. Therefore, it demonstrates that the overall sensitivity of the interferometer is improved by the common-mode design and reaches a single-digit picometer-level performance. The sensitivity characterization shows the capability of the interferometer as a highly sensitive optical readout system, especially in low-frequency applications such as inertial sensing area.

In the future, major error sources are to be investigated based on the preliminary measurement results, including laser frequency noises and temperature fluctuations. Moreover, the wavelength separation in the proposed system greatly depends on the reflectance and transmittance of corresponding spectrum for the narrow-bandwidth spectral filter. The effects from leakage and ghost reflection of the imperfect spectral filters are to be verified with analytical model and experiments. The system will eventually be tested in the vacuum chamber to reduce the acoustic noises, air turbulence, and refractive index fluctuations.

ACKNOWLEDGEMENT

The authors acknowledge financial support from National Science Foundation (NSF) grants PHY-2045579 and ECCS-1945832, and the support from National Aeronautics and Space Administration (NASA) through grant 80NSSC20K1723.

REFERENCES

[1] A. Hines, L. Richardson, H. Wisniewski et al., “Optomechanical inertial sensors,” Appl Opt, 59(22), G167-G174 (2020).
[2] S. M. Aston, and C. C. Speake, "An Interferometric Based Optical Read-out Scheme For The LISA Proof-Mass." 873, 326-333.
[3] T. Schuldt, H.-J. Kraus, D. Weise et al., "A High Sensitivity Heterodyne Interferometer as Optical Readout for the LISA Inertial Sensor." 873, 374-378.
[4] V. Wand, J. Bogenstahl, C. Braxmaier et al., “Noise sources in the LTP heterodyne interferometer,” Classical and Quantum Gravity, 23(8), S159-S167 (2006).
[5] V. Wand, F. Guzmán, G. Heinzel et al., [LISA Phasemeter development], (2006).
[6] B. S. Sheard, G. Heinzel, K. Danzmann et al., “Intersatellite laser ranging instrument for the GRACE follow-on mission,” Journal of Geodesy, 86(12), 1083-1095 (2012).
[7] K. Abich, A. Abramovici, B. Amparan et al., “In-Orbit Performance of the GRACE Follow-on Laser Ranging Interferometer,” Phys Rev Lett, 123(3), 031101 (2019).
[8] G. Heinzel, V. Wand, A. Garcia et al., [Investigation of noise sources in the LTP interferometer S2-AEI-TN-3028], (2008).
[9] M. Nofrarias, F. Gibert, N. Karnesis et al., “Subtraction of temperature induced phase noise in the LISA frequency band,” Physical review D, 87(10), 102003(8pp) (2013).
[10] F. Gibert, M. Nofrarias, N. Karnesis et al., “Thermo-elastic induced phase noise in the LISA Pathfinder spacecraft,” Classical and Quantum Gravity, 32(4), 045014(17pp) (2015).
[11] G. Heinzel, V. Wand, A. García et al., “The LTP interferometer and phasemeter,” Classical and Quantum Gravity, 21(5), S581-S587 (2004).
[12] M. Armano, M. Benedetti, J. Bogenstahl et al., “LISA Pathfinder: the experiment and the route to LISA,” Classical and Quantum Gravity, 26(9), (2009).
[13] K. S. Isleif, O. Gerberding, T. S. Schwarze et al., “Experimental demonstration of deep frequency modulation interferometry,” Opt Express, 24(2), 1676-84 (2016).
[14] K. Joo, E. Clark, Y. Zhang et al., “A compact high-precision periodic-error-free heterodyne interferometer,” Journal of the Optical Society of America A, 37(9), B11-B18 (2020).
[15] Y. Zhang, A. S. Hines, G. Valdes et al., “Investigation and Mitigation of Noise Contributions in a Compact Heterodyne Interferometer,” Sensors, 21(17), 5788 (2021).
[16] J. D. Ellis, [Field guide to displacement measuring interferometry] SPIE, Bellingham, 47-52 (2014).

Downloaded From: https://www.spiedigitallibrary.org/conference-proceedings-of-spie on 29 Jun 2022
Terms of Use: https://www.spiedigitallibrary.org/terms-of-use